New Plain Bearing Concept for Support of the Propeller Shaft in Pod-Drives of Large Ships

Dipl.-Ing. Sabine Gold

Institut für Fluidtechnik (IFD), Technische Universität Dresden, Helmholtzstraße 7a,
01069 Dresden, E-Mail: gold@ifd.mw.tu-dresden.de

Professor Dr.-Ing. Jürgen Weber

Institut für Fluidtechnik (IFD), Technische Universität Dresden, Helmholtzstraße 7a,
01069 Dresden, E-Mail: mailbox@ifd.mw.tu-dresden.de

Abstract

A new concept for drive-end bearings in pod-drives is presented. As roller bearings fail ahead of time, a dependable alternative for them is in demand. So the project aims at the combination of the hydrostatic with the hydrodynamic plain bearing principle in order to exploit their advantages. In addition to the requirement of high load-carrying capacity and reliability, good emergency operating features are needed. The paper describes the approach to develop the new bearing concept by means of numerical simulations as well as experimental investigations at a true-to-scale bearing test rig. New calculation methods were necessary to compute a combined hydrostatic/ hydrodynamic bearing flow. The simulation models are evaluated by test results.

KEYWORDS: pod-drive, radial plain bearing, Computational Fluid Dynamics (CFD), bearing test rig

1. Introduction

Pod-drives have gained a position of a major propulsion system for luxury cruise liners and ice going vessels as this concept has many benefits. One of which is the excellent manoeuvrability because the pod can be rotated 360° around its vertical axis. At the same time, rudders or long shafts inside the ship are not necessary. Space is saved inside the vessel hull, which means more freedom for ship design. In addition to very short stopping times and distances, pod-drives can reduce fuel consumption. **Figure 1** shows the propulsion system of a cruise liner with three pod-drives.

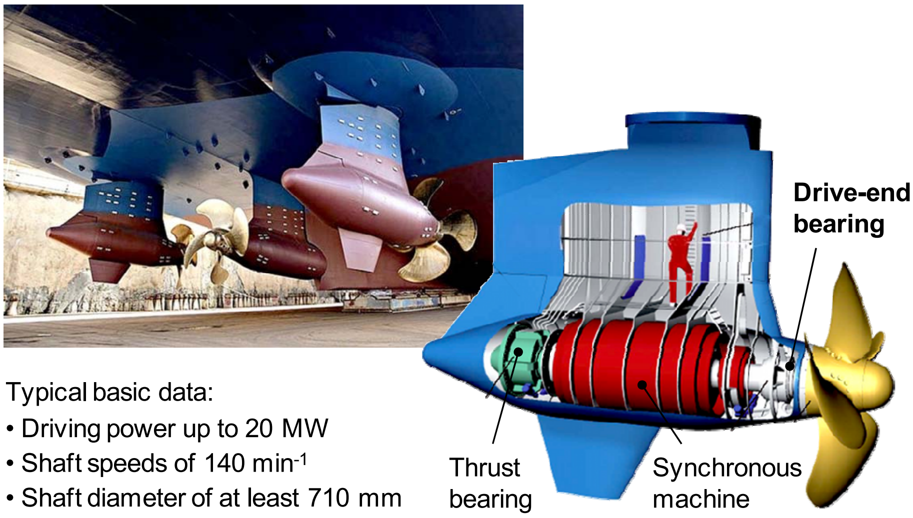

Figure 1: Cruise liner with pod-drives

However, there are disadvantages, too. The pod's slewability causes unsteady flows with highly dynamic load components that significantly reduce the durability of the shaft bearings. State-of-the-art is the use of roller bearings for support of the propeller shaft. Failures occur especially at the drive-end bearing (see figure 1), which always means dry dock and high financial losses. So the aim is to develop a new reliable and robust bearing concept with a long operating life in order to increase the docking intervals of the ships.

For this purpose, the joint research project HYDROS was initiated, funded by the German Federal Ministry of Economics and Technology. Cooperation partners are Blohm + Voss Industries (BVI) in Hamburg, Germany, ABB Marine in Helsinki, Finland, the Chair of Mechanical Engineering Design/CAD at the University of Rostock, Germany, as well as the Institute of Lightweight Engineering and Polymer Technologies (ILK) and the Institute of Fluid Power (IFD) at TU Dresden, Germany.

The objective of this research project is the computation and experimental verification of combined hydrostatic/hydrodynamic radial plain bearings for propeller shafts in pod-drives. Therefore, several calculation programmes as well as two test rigs are employed. In addition to a true-to-scale bearing test rig - representing the conditions of the pod-drive - a lab test stand for detailed investigations is available. Because of the bearing's size, experimental testing is very time consuming and expensive. There was the need to reduce development efforts and costs by evaluating the capability of different technical solutions using simulation. So, comprehensive theoretical studies were carried out before the production and investigation of prototypes. Different analytical and numerical approaches were used to gain more reliability in predicting the bearing's performance.

2. Hydrostatic/hydrodynamic plain bearing concept

Plain bearings offer numerous advantages such as high stiffness and damping or low friction and wear. Thus, they are an alternative to roller bearings in pod-drives. However, supporting a pod's propeller shaft constitutes a new field of application for plain bearings. This implies the following requirements for drive-end bearings in pod-drives:

- Reliable operation and long operating life
- High load-carrying capacity also at low rotational speeds
- Good emergency operating features in case of a failure of the pressure supply
- Energy-efficiency

Hydrostatic plain bearings meet the first two demands very well, but have a high risk of damage in case of a pressure supply breakdown and are very power consuming. In contrast, hydrodynamic plain bearings require no high pressure supply. So they work more energy-efficient. Moreover, they have very good emergency operating features. The idea is to combine the advantages of both bearing principles in order to create a robust and energy-efficient hybrid bearing for pod-drives.

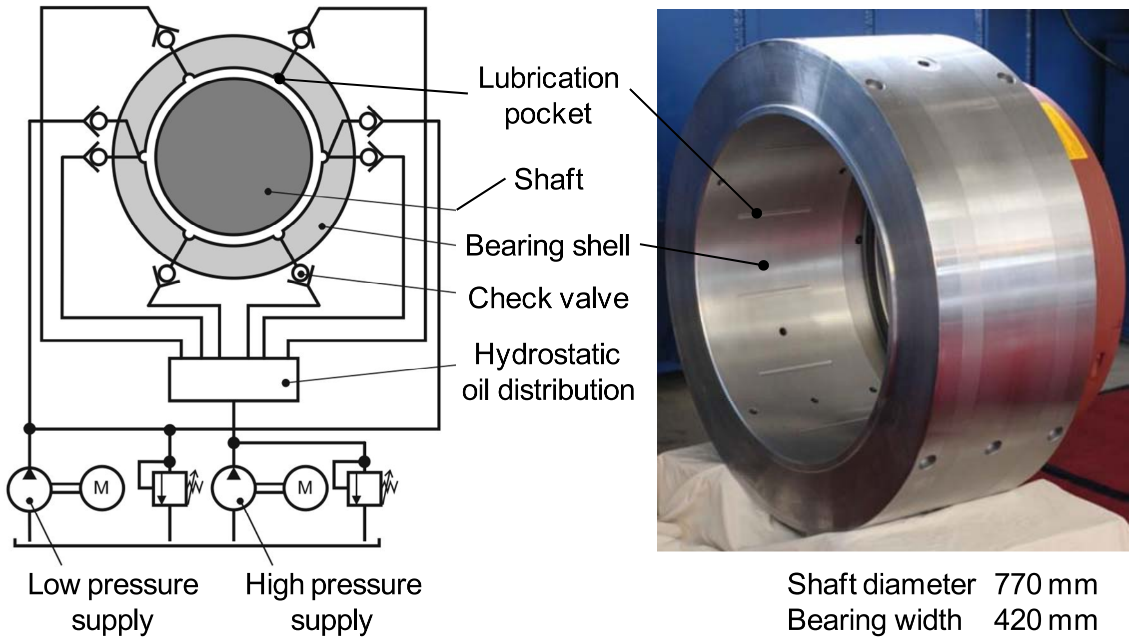

Figure 2: Concept of the hybrid plain bearing /1/ and first prototype

Figure 2 shows the structure of the hybrid bearing concept /1/ as well as the bearing ring of the first prototype. The bearing is characterized by a cylindrical sliding surface interrupted by twelve small lubrication pockets, actually no more than grooves. Each pocket is connected to the high pressure supply for operating the bearing hydrostatically. In the feed line of each pocket, a check valve is installed that prevents the oil's backflow to guarantee hydrodynamic pressure built-up. Thus, the bearing can work in hydrodynamic operating mode with low supply pressure if the shaft speed is sufficient. The large sliding surface also prevents the contact of rotating shaft and bearing shell in case of a missing supply pressure.

Hydrostatic bearings need a device for the distribution of the oil among the bearing pockets. Flow restrictors, which are positioned upstream the pockets, are used for this purpose. However, capillaries as classical restrictors cause high flow rates of about 100 l/min in bearings of this size. Load-dependent restrictors decrease the oil flow without performance losses. They control the volume flow into the pockets, depending on the force applied to the bearing and the pressure in the pocket respectively. One example are membrane restrictors, which adjust the fluid flow into a hydrostatic device proportionally to the load pressure. They deliver an increasing flow rate into the pocket when the pocket pressure rises. Unloaded pockets only receive a small amount of oil. In this way, a lot of volume flow can be saved. The mechanical design and the functionality of membrane restrictors are described in /2/. Of course, further flow resistances, e.g. proportional valves, were also investigated during the project.

3. Numerical investigations

There are differing design guidelines and calculation methods for hydrostatic and hydrodynamic bearings respectively. For computing a combined hydrostatic/ hydrodynamic bearing flow, the further development of existing tools was necessary. The project partners followed up different approaches in order to predict the bearing's performance. The integral version of the Reynolds equation was derived concerning the hybrid bearing's geometry to calculate the pressure distribution in the bearing gap analytically. Two numerical programmes were employed for more detailed computations of the bearing flow using the enhanced Reynolds equation and the Navier-Stokes equations. Furthermore, FEM software was used to gain information about the deformation of the bearing shell under load.

The most important software tools for design and investigation of the new bearing concept are the two numerical programmes SIRIUS and ANSYS FLUENT. The academic programme SIRIUS, which was developed at the University of Rostock /3/, performs the two-dimensional calculation of the planar gap flow using the enhanced Reynolds equation. The commercial CFD code FLUENT is used to run three-dimensional simulations of the complex flow field in the plain bearing solving the Navier-Stokes equations. Both programmes complement each other. On the one hand, SIRIUS is suitable for the calculation of a large number of variants as it is very fast owing to many simplifications. On the other hand, the FLUENT, which has been validated many times, provides more reliability and allows the computation of flow mechanical details in addition to the bearing's operational behaviour. Both approaches are described more precisely and compared in /4/.

This paper focuses on three-dimensional calculations with FLUENT. The CFD software was used to analyse several hybrid bearing concepts concerning load-carrying capacity and power requirement in order to determine the most promising solution. In contrast to the simplified 2D SIRIUS model, the geometry of the lubrication gap between bearing shell and shaft is modelled in detail in FLUENT, including the shape of the bearing pockets as well as the inlet bores. Thereby, advantage is taken of the bearing's symmetry in axial direction to reduce the size of the model and the numerical effort respectively. The gap height is discretised with eight cells. Altogether, the CFD model contains about 1.3 million hexahedral elements. Important modelling parameters are summarised in **table 1**.

Parameter	Value
Shaft diameter	d = 770 mm
Bearing width	b = 420 mm
Bearing clearance	s = 0.6 mm
Shaft speed	n = 0 .. 140 min^{-1}
Nominal load force	F_L = 0.9 MN
Maximum load force	$F_{L.max}$ = 2.4 MN
Supply pressure	p_0 = 220 bar
Kinematic oil viscosity	v = 100 cSt
Oil temperature	T_{Oil} = 40 °C

Table 1: Parameters for CFD calculations of hybrid bearing

Figure 3 illustrates the modelling of the bearing in FLUENT. The volume flow into the lubrication pockets is defined as boundary condition using the flow function of the respective restrictor. Both the restrictor and the check valve are implemented in a user-defined function (UDF) within the flow inlet. Using UDFs is a very flexible possibility to model different flow resistances with low effort by changing the characteristic curve. See /5/ for a more detailed description of the simulation model.

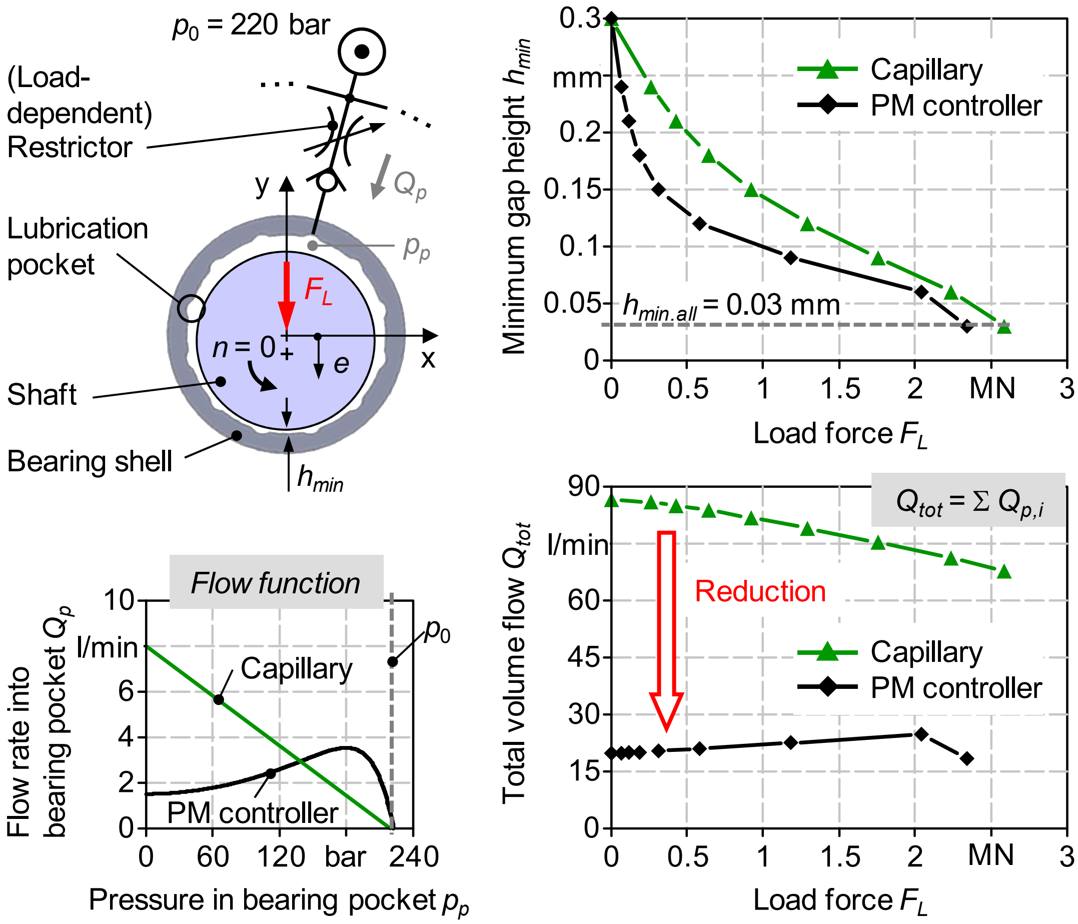

Figure 3: FLUENT modelling and results – comparison of bearing with capillaries and PM controllers

As an example, the static performance of the hybrid bearing in hydrostatic operating mode for two types of volume flow control is compared in figure 3: the conventional constant flow resistance capillary and the load-dependent membrane restrictor PM controller. Static CFD calculations were carried out for a load force range of F_L = 0 .. 2.4 MN. FLUENT computes the pressure and velocity distribution of the bearing flow. The respective values for shaft position, bearing force and flow rate characterise the steady state behaviour of the bearing and allow an evaluation of the flow control concepts. As expected, the bearing with capillaries has a very high volume flow demand up to Q_{tot} = 86 l/min. Using load-dependent restrictors for the reduction of the flow rate into unloaded pockets causes a remarkable decrease of the total volume flow and thus of the hydraulic power consumption (see diagram below on the left in figure 3). The bearing with PM controllers only needs a maximum volume flow of Q_{tot} = 25 l/min. This means a reduction of about 30 %. Certainly, the volume flow strongly depends on fluid temperature and viscosity respectively, as we have laminar flow resistances here (capillary, PM controller, bearing gap). Consequently, highly viscous oil of the viscosity class ISO VG 100 was chosen for operating the bearing. Despite the big difference in the flow rate, both concepts have similar load-carrying capacities. The upper diagram shows the remaining minimum gap height h_{min}, the size of which depends on the load force. The gap height is h_{min} = 0.3 mm at a centric shaft position. It is reduced in load direction by increasing the bearing load. The bearing with capillaries is stiffer than the one with PM controllers at low forces as the larger decrease of the black curve implies. However, both bearing concepts have a similar stiffness and load-carrying capacity at higher loads. An allowable minimum gap height of $h_{min.all}$ = 0.03 mm was defined for the maximum bearing load of 2.4 MN. Both bearings can bear this load in compliance with the limit value for h_{min}.

Of course these results are just a small excerpt from a wide variety of calculations. The operational behaviour of several bearing designs and control concepts was computed for different static and dynamic load cases. By means of comprehensive simulation studies, the functional capability of the new hydrostatic/hydrodynamic plain bearing concept was proved. The hybrid bearing meets the requirements concerning load-carrying capacity, reliability and power consumption. The design for a first prototype was derived from this knowledge. Three flow control concepts were chosen for the investigation at the test rig.

4. Experimental studies

4.1. Bearing test rig

A true-to-scale bearing test rig was designed and constructed to prove the different bearing concepts as well as to validate the simulation models. **Figure 4** illustrates its basic layout. The pod's propeller loads are simulated by hydraulic cylinders driven by an electronic control system. Two radial actuators apply variable radial forces to the test bearing. They are arranged in a 90° angle to add their forces and reach the maximum load of $F_{L.max}$ = 2.4 MN at the test bearing. A third hydraulic cylinder (axial actuator) is used for the shaft's axial displacement. The rotational movement of the shaft is realized by a frequency-converter-driven asynchronous motor.

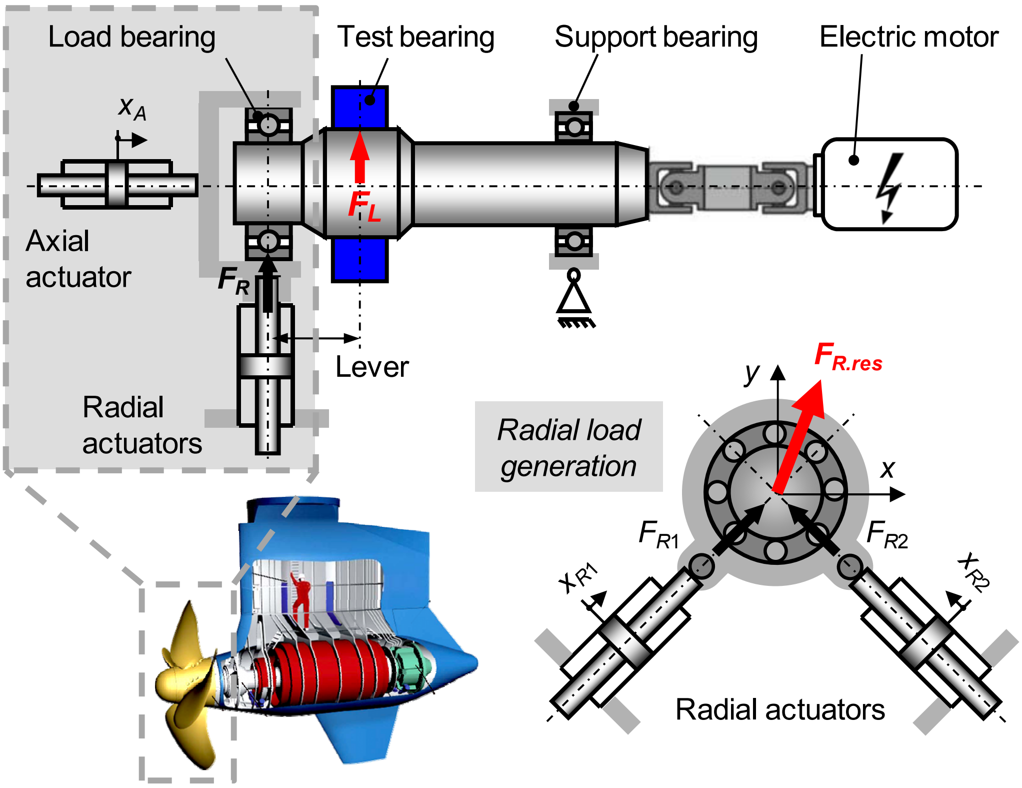

Figure 4: Structure and load generation of the true-to-scale bearing test rig

Extensive measuring equipment was installed at the test stand to investigate the operational behaviour of the prototype. Sensors are available to record the

- Height of the bearing clearance at eight points
- Pressure in lubrication pockets, supply system, etc.
- Total volume flow and single flow into one pocket
- Temperature of oil, shaft and bearing shell

Figure 5 shows the bearing test rig in the test hall in Dresden (see photo above). Its installation area amounts to 9 x 4 m² and is about 3 m high. The test stand has a total weight of 45 t and a driving power of 250 kW.

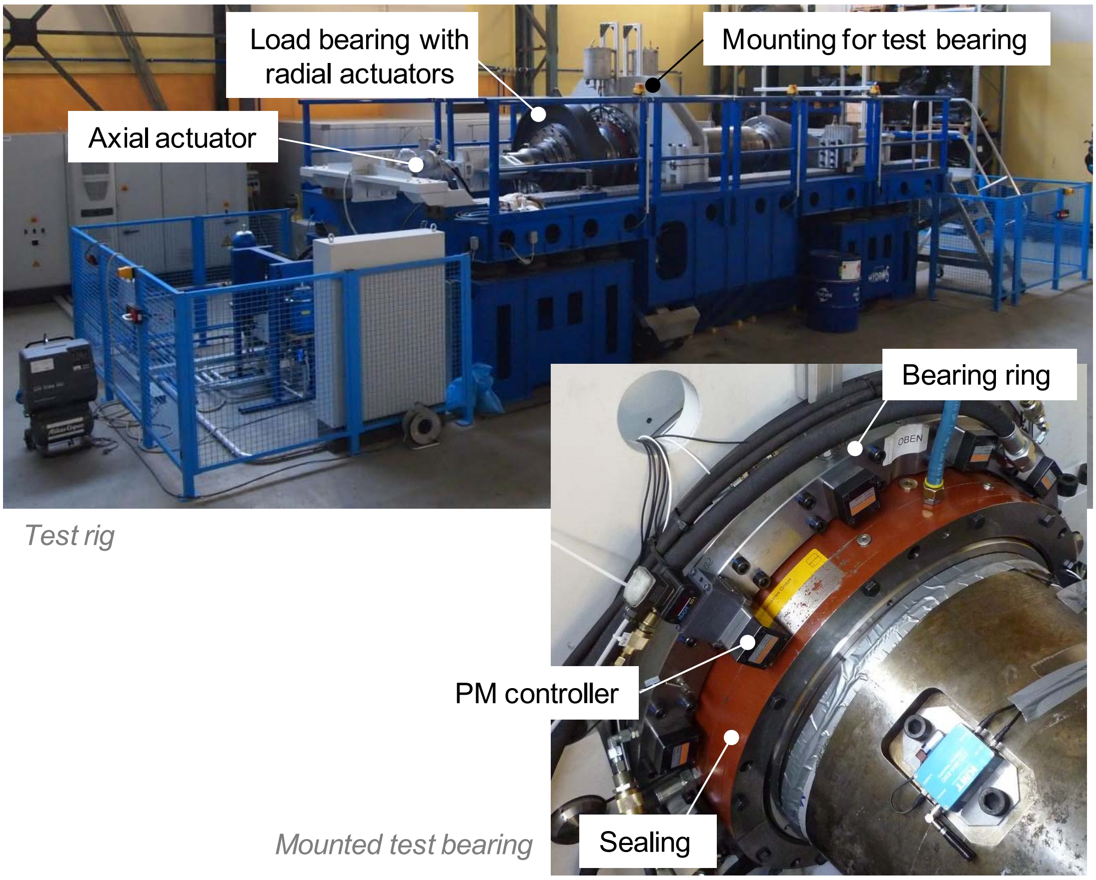

Figure 5: Bearing test rig and first prototype with PM controllers

The first bearing prototype was designed modularly to provide the opportunity of examining several flow control concepts with one bearing. Figure 5 (photo on the right) shows the PM controllers mounted at the front of the bearing ring. They can be easily replaced by other restrictors. In this way, three different control concepts will be investigated and compared to determine one preferred variant for a second prototype.

4.2. Measurement results

As mentioned above, a lot of measurement values are recorded to investigate the bearing’s performance. **Figure 6** shows the first results for the prototype with PM controllers in hydrostatic operating mode. Load-carrying capacity and power requirement are illustrated by the minimum gap height h_{min} as well as the total volume flow through the bearing Q_{tot}, which depends on the load force F_L. The minimum gap height - measured by non-contact eddy current sensors - decreases with growing load, see the diagram on the left (blue solid line). At a load force of 2.1 MN, a minimum gap height of h_{min} = 0.125 mm was left in the bearing centre. This means that a higher load could theoretically be borne. Nevertheless, as the shaft tilts in the bearing ring, a safety factor must be considered. In this case, a gap height of 0.125 mm in the middle means a minimum height of h_{min} = 0.06 mm at the edge of the bearing shell. This value is decisive to avoid mixed friction or solid state contact.

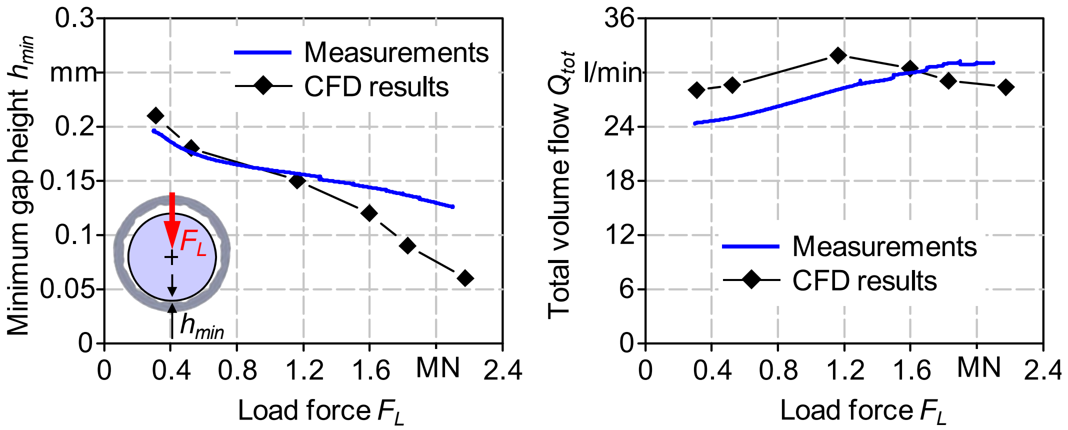

Pressure distribution for

Load force	F_L = 1.8 MN
Shaft speed	n = 0
Supply pressure	p_0 = 160 bar
Oil – visc. class	ISO VG 100
Av. oil temperature	T_{Oil} = 29 C

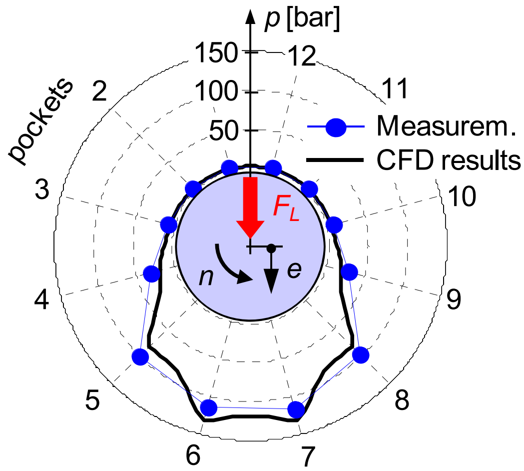

Figure 6: Comparison of measurements and CFD results for bearing with PM controllers: static operational behaviour and pressure distribution

The right diagram in figure 6 displays the total volume flow through the bearing. The increase results from the flow function of the PM controller, compare also figure 3. A higher load means a higher pocket pressure, which leads to a rise of the flow rate into the pocket. Nevertheless, a volume flow of 24 to 31 l/min is very low for a hydrostatic bearing of this size. With a supply pressure of 160 bar the hydraulic power demand is about 8 kW.

Moreover, the CFD results computed for this bearing configuration are shown in the diagrams (black symbols) in order to compare calculation and measurement and to evaluate the simulation model. The minimum gap height matches very well for small loads. There is a growing difference between blue curve and black rhombi at forces of $F_L \geq 1.2$ MN. The load-carrying capacity of the prototype is better than the one of the simulation model. The reason for this will be discussed below. Calculated and measured flow rates disaccord slightly in the load dependency, but qualitative curve progression and dimension fit satisfactorily. The reason for this discrepancy can be the simplified modelling of the PM controllers or the assumption of a constant oil temperature and viscosity in FLUENT. This fact requires some further research. Additional experimental investigations concerning temperature dependency of the flow rate are necessary, too.

Beyond that, the pressure distribution in the bearing at a load force of 1.8 MN is depicted in the circle graph in figure 6. The measured pocket pressures (blue points) are contrasted with the computed pressure profile on the shaft surface (black solid line). The pressure distribution is symmetric to the load direction as the shaft does not rotate. The diagram shows a very good correlation between simulation and experiment. However, a difference becomes visible, too. The pressure in pockets 6 and 7 is clearly higher than in 5 and 8 in the CFD results. In contrast, the measurement gives similar pressure values in these four pockets. The pressure distribution homogenises. It can be concluded that the bearing ring widens under load. As a consequence, there is the same gap height between shaft and bearing ring in a wider range of the circumference. This leads to similar pocket pressures. So, a better load-carrying capacity is achieved at higher loads because of the wider “pressure pad”, as the results show. This effect does not occur in the FLUENT calculations (see diagram for h_{min} in figure 6) as the bearing shell is modelled as ideal stiff solid body without deformation. Nevertheless, this deficit of the simulation model delivers more safety in designing the bearing. If the CFD results meet the requirements, the prototype works in any case. Finally, it should be noticed that the required maximum load of 2.4 MN cannot be reached with this bearing configuration. PM controllers are only available up to a supply pressure of p_0 = 160 bar at the moment. This is not sufficient for the maximum load force. Anyway, the functionality of the control concept “Hybrid bearing with PM controller” was proved and will be investigated and developed further on.

5. Conclusions

Combining the contrasting principles of hydrostatic and hydrodynamic plain bearings is a new approach to achieve a robust and reliable drive-end bearing for pod-drives of large ships. In the research project HYDROS the theoretical basics were created to describe the combined hydrostatic/hydrodynamic bearing flow. New simulation tools were developed to compute the static and dynamic operational behaviour of several design drafts and flow control concepts of the new hybrid bearing. The bearing's performance was predicted in comprehensive simulation studies. Different concepts were evaluated and compared in order to find promising solutions without any experimental effort. Of course, a true-to-scale bearing test rig was constructed for investigating prototypes under realistic conditions. First measurement results confirm the numerical calculations quiet well. Owing to the large use of complementary simulation tools, high reliability was achieved for determining the bearing flow. The simulation models will be improved on basis of the experimental investigations. Further tests are necessary for the verification of the simulation models as well as the adequate examination of the prototypes. Two results will be realized at the end of the project. A functional prototype of a load-controlled hybrid plain bearing will be available that meets the defined requirements. In addition, a verified simulation tool will exist for designing hybrid bearings for various applications.

6. Acknowledgements

The presented research activities are part of the project "HYDROS - Lastgesteuertes hydrostatisches Lager". The authors would like to thank the German Federal Ministry of Economics and Technology and the Project Management Jülich for their financial support.

Supported by:

Federal Ministry
of Economics
and Technology

on the basis of a decision
by the German Bundestag

7. References

/1/ Wegmann, R. Radial plain bearing with optional hydrostatic and/or hydro-dynamic function. Patent application WO 2010/103100 A1. Deutsches Patent- und Markenamt. 2010.

/2/ Winterschladen, M. Verfahren zur ganzheitlichen Auslegung von hydrostattischen Führungen und Lagern. Dissertation, RWTH Aachen, Germany. 2008.

/3/ Wegmann, R. Erweiterung der hydrodynamischen Schmiertheorie durch Einbeziehung des Unterdruckgebietes in die Berechnung instationär belasteter Gleitlager. Dissertation, Universität Rostock, Germany. 1978.

/4/ Gold, S.; Weber, J.; Wegmann, R.; Brökel, K.: Auslegungs- und Simulationsstrategien für hydrostatisch-hydrodynamische Hybridlager im Schwerlastbereich. Conference paper. VDI-Fachtagung Gleit- und Wälzlagerungen. Schweinfurt. 2011. VDI-Berichte 2147.

/5/ Gold, S.; Weber, J.; Wegmann, R.: New hydrostatic/hydrodynamic plain bearing concept for heavy duty applications. Conference paper. SICPF'11. Tampere. 2011.

8. Nomenclature

e	Shaft eccentricity	mm
F_L	Bearing load force	MN
F_R	Load force of radial actuator	MN
h_{min}	Minimum gap height	mm
n	Shaft speed	min^{-1}
p_p	Pressure in bearing pocket	bar
p_0	Supply pressure	bar
Q_p	Volume flow into bearing pocket	l/min
Q_{tot}	Total volume flow	l/min
T_{Oil}	Oil temperature	°C
x	Cylinder stroke	mm
v	Kinematic oil viscosity	cSt